Assessing the Quality and Stability of Photogrammetric Point Clouds Derived from Stereo UAV Imagery

Version 2015-03-31

Prepared for:
Delinda Ryerson
Application Centre, Alberta Biodiversity Monitoring Institute

Prepared by:
Greg McDermid
Department of Geography, University of Calgary

1.0 Assessing the Quality and Stability of Photogrammetric Point Clouds Derived from Stereo UAV Imagery

1.1 Introduction

Near-surface imaging from Unmanned Aerial Vehicles (UAVs) represents an important development in remote-sensing science, bridging the gap between ground-based observations and high-altitude image data acquired from satellites and piloted aircraft. While airborne platforms have always played a key role in the field of remote sensing, modern UAVs have several important advantages over traditional aerial platforms, including flexible low-cost sensor deployment, safe near-surface operation, and extraordinarily high-resolution imaging capabilities. However, the technology is relatively new and subject to a variety of operational uncertainties.

One of the most promising emerging applications of UAV technology involves the production of detailed elevation data from stereoscopic image pairs. While the principles of photogrammetric surface extraction from stereoscopic parallax have been around for decades (e.g. Wolf, 1983), recent advances such as the development of multi-view stereopsis (e.g. Furukawa and Ponce, 2010) and other automatic approaches to image matching have enabled the rapid extraction of 3D surfaces through bundle adjustment. By applying these procedures to digital near-surface imagery, modern software packages such as Bundler (Snavely et al, 2007), EOS Systems PhotoModeler, Microsoft Photosynth, and Agisoft Photoscan have been shown to produce elevation data sets comparable to those generated by laser scanning (Haala, 2009; Pierrot-Deseilligny and Cleary, 2011; Lisein et al, 2013; Dandois and Ellis, 2013). While lacking the multiple-return and canopy penetrating abilities of LiDAR, photogrammetric point clouds derived from optical UAV imagery offer an attractive, low-cost approach to 3D imaging, with emerging applications in rangeland management (Laliberte et al, 2011), agriculture (Honkavaara et al, 2013), forestry (Balstavias et al, 2008; Dandois et al, 2010), archaeology (Lin et al, 2011), and microtopography (Lucieer et al, 2014), amongst others.

While the quality of photogrammetric surface models is nominally dependent on basic flight characteristics, the image-matching algorithms at the heart of modern processing routines are dependent on a variety of image quality and target characteristics (Haala, 2009; White et al, 2013) that raise a variety of questions surrounding the appropriate conditions for acquiring UAV-based imagery for photogrammetric applications. For example, what is the impact of solar-illumination conditions on the quality of photogrammetric point clouds? Do data sets acquired under direct-light conditions compare favorably to those acquired under diffuse light? What effect do target complexity (e.g. land cover, topography), UAV platform (fast-moving fixed-wing, slow-moving copters), and sensor payload (inexpensive compact/subcompact camera, full-featured mirrorless/dSLR) have on the accuracy and stability of results? While previous studies have evaluated the quality of topographic data derived from satellites (Kaab, 2002; Aguilar, 2014), piloted aircraft (Adams and Chandler, 2002; Haala, 2009), and UAVs (Harwin and Lucieer, 2012; Dandois and Ellis, 2013), there remains an overall shortage of relevant work in this rapidly evolving field.

1.1.1 Objectives

The purpose of this research is to perform a systematic evaluation of the impact of target complexity and illumination conditions on the quality and stability of point clouds extracted from stereo imagery acquired by UAVs. We measured the accuracy and completeness of digital surface models (DSMs) acquired under a variety of conditions against reference LiDAR data at two different field locations in Alberta, Canada. Our purpose is to gain insight into the factors affecting the quality of topographic models acquired from UAV data, and to highlight the optimal (and sub-optimal) conditions for high-quality data acquisition.

This document is intended to provide an interim report of activities that took place in fiscal year 2014, including an overview of the study areas, a description of field and flight protocols followed, and an update of on-going data analysis.

1.2 Study Areas

We established two field sites to conduct our flight experiments: one located in the rangeland portion of Alberta, Mattheis Ranch, and another in the foothills: Beaver Mines (Figure 1).

1.2.1 Mattheis Ranch (Rangeland)

The Mattheis Ranch property is located near the town of Duchess, Alberta, 150 km east of Calgary (Figure 2). The ranch is part of the University of Alberta's Rangeland Research Institute, and is located in the Dry Mixedgrass natural subregion (Natural Regions Committee, 2006). The property is comprised primarily of rangeland, though portions of cultivated farmland are also present. The ranch contains a variety of natural ecosystems and habitats, including riparian areas along the Red Deer River and Matziwin Creek, and several large wetlands.

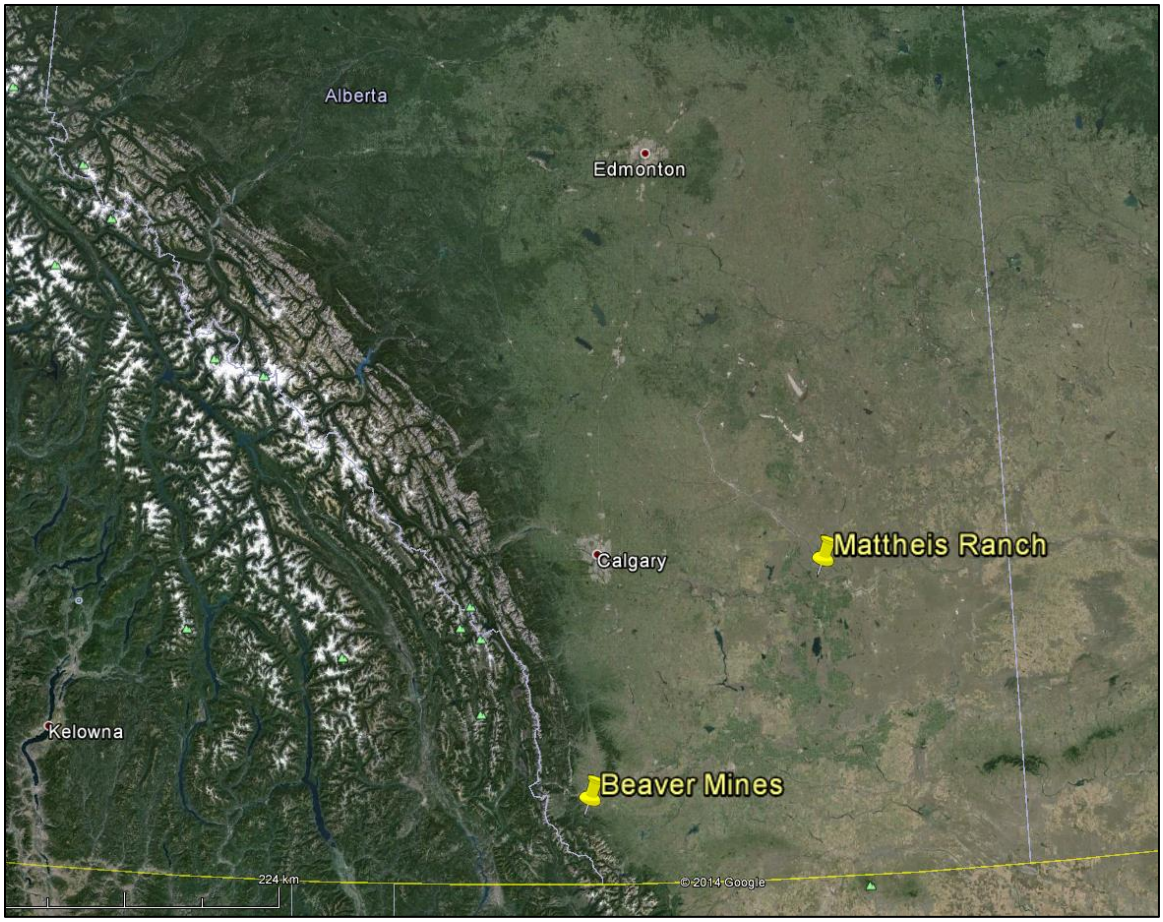

Figure 6.1: Location of Mattheis Ranch (rangeland), Beaver Mines (foothills) study areas in southern Alberta.

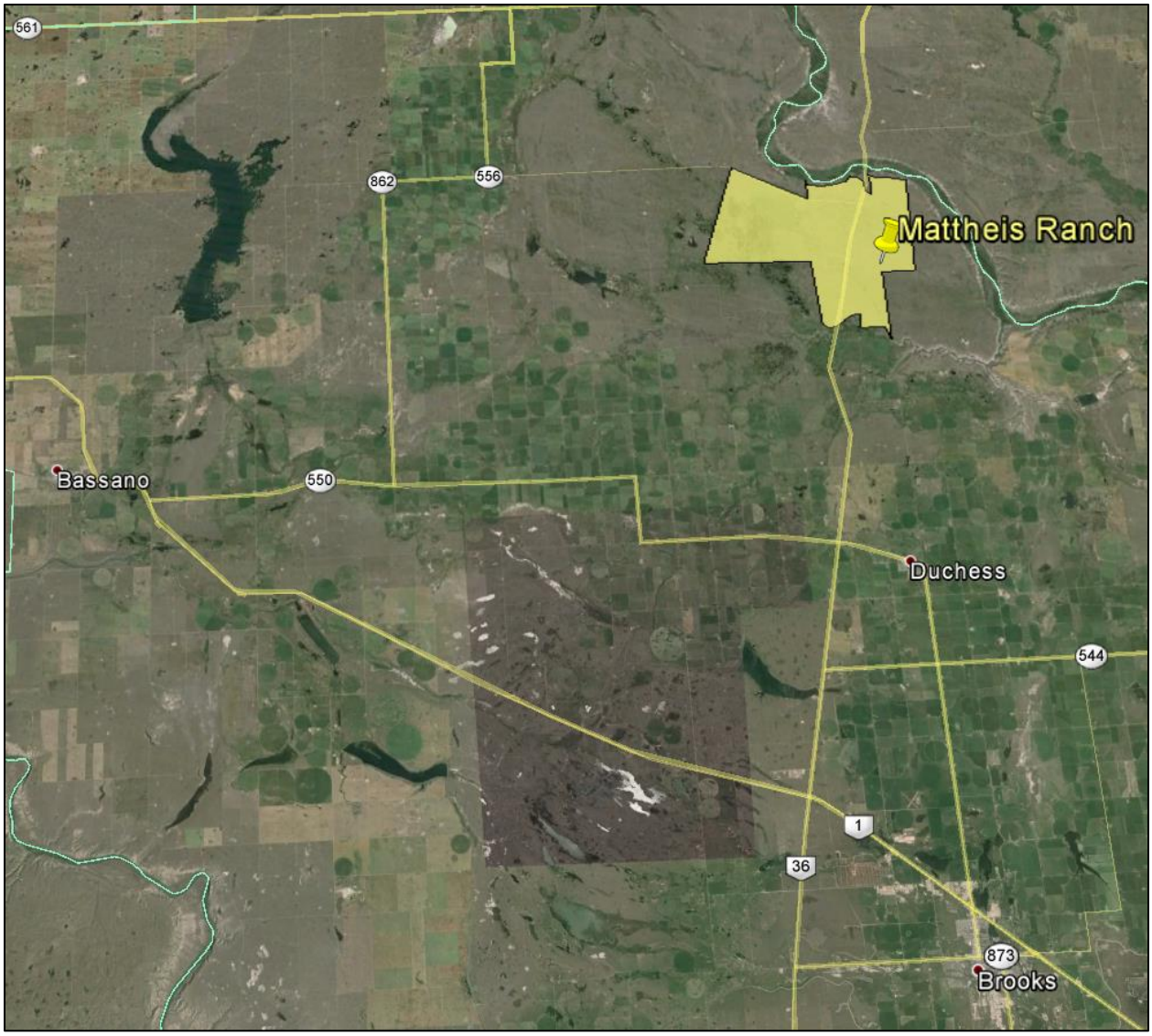

Figure 6.2: The Mattheis Ranch study area is located near the town of Duchess, Alberta, 150 km east of Calgary.

1.2.2 Beaver Mines (Foothills)

The Beaver Mines property is located near the town of Pincher Creek, 180 km south of Calgary (Figure 3). The ranch is privately owned by Stuart McDowall, though a small cabin on the property is leased by a third party. The property is located in the Montane natural subregion (Natural Regions committee, 2006), and is comprised of a complex mix of rangeland and mixed forest, with wetland and riparian areas occurring along Beaver Mines Creek in the valley bottom. The region is topographically complex, with underlying foothills relief accentuated by eskers and other glacial landforms.

Figure 6.3: The Beaver Mines study area is located near the town of Pincher Creek, Alberta; 180 km south of Calgary.

1.3 Data Sets

1.3.1 UAV Imagery

High-spatial-resolution imagery were acquired with a fixed-wing Quest Q-Pod with a Sony NEX 7 over roughly 1-km^2 sample blocks located within both study areas. Imagery were acquired systematically in order to acquire complete aerial surveys (80% endlap, 50% sidelap) under both direct- and diffuse-light conditions for solar-elevation angles ranging from 15° to ~60. Our plans called for a total of 8 successful imaging flights (4 direct-light, 4 diffuse-light) over both study areas.

1.3.2 Ground Control

While relative rectification on an arbitrary coordinate system can be achieved without the collection of ground control points (GCPs; Turner et al, 2014), accurate absolute rectification requires high-quality

GCPs (X, Y, and Z). To achieve this, we laid out coloured buckets to serve as visible ground control across each study area. The locations of these GCPs was established with survey grade GPS.

1.3.3 Atmosphere and Illumination

Atmospheric and illumination observations relevant to the amount and quality of shortwave solar radiation available for photography were acquired systematically throughout each flying day. We measured the total and diffuse components of shortwave radiation with LI-COR LI-200 pyranometers attached to a LI-1400 data logger, logging at 1-minute intervals. One pyranometer was placed behind a sun shade to measure diffuse radiation, while the other was placed with an unobstructed view of the sky to measure total radiation. The proportion of diffuse radiation (% diffuse) available during each flight was calculated as the simple ratio of the two instantaneous measurements, and averaged across the duration of the flight. The solar elevation angle for each flight was estimated using the NOAA Solar Calculator (http://www.esrl.noaa.gov/gmd/grad/solcalc/), with inputs acquired from image metadata and flight logs.

1.4 Field Protocol

We established a careful field protocol in order to establish a clear methodology for field crews to follow and address any subjectivity in field observations. In all cases, field-crew safety and uniformity in data collection is the ultimate objective.

1.4.1 Field Teams

A complete UAV crew consists of between three and five team member, at least three of which (all except the Field Manager and Ground Control Manager) must be on-site during flights. The roles and responsibilities of each crew member are summarized below:

1.4.2 Field Manager

The field managers is responsible for the overall safety and management of the field crew, security of the data, and maintenance of field instruments. This individual will make daily decisions designed to ensure the successful execution of the field plan.

1.4.3 UAV Commander

The UAV commander is responsible for the successful execution of each flight mission, navigation planning, and flight logs (Appendix I). The Commander ensures that the computing resources, GPS, and ancillary (ie, non-aircraft) equipment are serviceable and available for each mission. On return from the mission, the Commander returns all such equipment to the lab, and reports damaged/missing pieces.

1.4.4 UAV Pilot

The UAV Pilot is responsible for the complete control of the UAV during flight. The pilot is responsible for pre-flight preparations, risk assessment, and UAV maintenance. The pilot has the authority to give commands during flight to spotters/ground crew, and works collaboratively with the UAV Commander

to ensure the safe completion of each flight. The pilot ensures that the UAV is packed, serviceable, and available for each mission, and returns all such equipment to the lab on completion.

1.4.5 Spotter

The Spotter assists the pilot in the duties associated with collision avoidance, and informs the pilot of any notable sightings or sounds. The spotter keeps eyes on the UAV at all times during flight, and is responsible for aircraft retrieval during a planned (or unplanned) landing. The Spotter will also take responsibility for the set up and maintain the pyranometer equipment, and the preliminary completion of flight logs (Appendix I).

1.4.6 Ground Control Manager

The Ground Control Manager is responsible for the layout and survey of GCPs, orientation of aircraft into the wind, and the location/height of datum and emergency rally point (ERP). During flights, the Ground Control Assistant can assist the Spotter, if available.

1.5 Preliminary Results and Next Steps

A total of 16 data sets were acquired over the two study areas: 8 at Mattheis Ranch and 8 at Beaver Mines (Table 1). Each set was processed using AgiSoft PhotoScan into photogrammetric points clouds and geometrically corrected to UTM Zone 11 NAD 83. Preliminary results reveal the variability of point-cloud quality, canopy penetration, and completeness as a function of photographic light quality. High-solar-elevation, direct-light conditions tended to lower-quality point clouds, particularly in the low-relief Mattheis Ranch site. By contrast, low-solar-elevation direct-light conditions produced lower-quality point clouds in the complex terrain of Beaver Mines. Diffuse-light conditions tended to produce better point clouds in both sites. A complete quantitative analysis is currently underway, and a full manuscript is anticipated for FY 2015.

Table 6.1: Summary of data sets acquired at Mattheis Ranch (MR) and Beaver Mines (BM).

Flight	Location	Date	Time	Camera	Flight Timing	Solar Elevation	Light (% diffuse)
BM-15-DIR	Beaver Mines	6/20/2014	09h00m	NEX-7 (16mm)	08:56-09:08	20.39-22.3	18.9
BM-0-DIF	Beaver Mines	7/28/2014	07h00m	NEX-7 (16mm)	07:09-07:23	0.65-2.46	40.4
BM-15-DIF	Beaver Mines	7/28/2014	08h30m	NEX-7 (16mm)	08:32-08:45	12.69-14.74	33.2
BM-30-DIF	Beaver Mines	7/28/2014	10h30m	NEX-7 (16mm)	10:29-10:42	31.5-33.58	31.9
BM-45-DIF	Beaver Mines	7/28/2014	12h00m	NEX-7 (16mm)	12:05-12:18	46.25-48.05	34.5
BM-60-DIR-A	Beaver Mines	7/28/2014	13h30m	NEX-7 (16mm)	13:26-13:39	55.94-57.04	7.4
BM-60-DIR-B	Beaver Mines	7/28/2014	14h30m	NEX-7 (16mm)	14:35-14:49	59.62-59.64	8.6
BM-45-DIR	Beaver Mines	7/28/2014	17h30m	NEX-7 (16mm)	17:35-17:44	44.31-42.98	7.8
MR-45-DIR	Mattheis Ranch	7/9/2014	11h30m	NEX-7 (16mm)	11:38-11:49	45.77-47.34	7.1
MR-60-DIR	Mattheis Ranch	7/9/2014	14h30m	NEX-7 (16mm)	14:28-14:39	61.41-61.4	6.8
MR-45-DIR	Mattheis Ranch	7/9/2014	17h30m	NEX-7 (16mm)	17:23-17:36	46.43-44.55	8.2
MR-30-DIR	Mattheis Ranch	7/9/2014	18h30m	NEX-7 (16mm)			
MR-15-DIR	Mattheis Ranch	7/9/2014	20h00m	NEX-7 (16mm)			
MR-15-DIF	Mattheis Ranch	8/21/2014	09h00m	NEX-7 (16mm)	09:02-09:11	14.27-15.68	48
MR-30-DIF	Mattheis Ranch	8/21/2014	10h30m	NEX-7 (16mm)	10:25-10:34	27.18-28.55	45.6
MR-45-DIF	Mattheis Ranch	8/21/2014	12h40m	NEX-7 (16mm)	12:34-12:43	44.43-45.35	51.6

References

Adams, J.C., & Chandler, J.H. (2002). Evaluation of lidar and medium scale photogrammetry for detecting soft-cliff coastal change. Photogrammetric Record, 17, 405-418

Angel Aguilar, M., del Mar Saldana, M., & Jose Aguilar, F. (2014). Generation and Quality Assessment of Stereo-Extracted DSM from GeoEye-1 and WorldView-2 Imagery. IEEE Transactions on Geoscience and Remote Sensing, 52, 1259-1271

Dandois, J.P., & Ellis, E.C. (2010). Remote Sensing of Vegetation Structure Using Computer Vision. Remote Sensing, 2, 1157-1176

Dandois, J.P., & Ellis, E.C. (2013). High spatial resolution three-dimensional mapping of vegetation spectral dynamics using computer vision. Remote Sensing of Environment, 136, 259-276

Furukawa, Y., & Ponce, J. (2010). Accurate, Dense, and Robust Multiview Stereopsis. Ieee Transactions on Pattern Analysis and Machine Intelligence, 32, 1362-1376

Haala, N. (2009). Combeck of digital image matching. Photogrammetric Week, 9, 289-301

Harwin, S., & Lucieer, A. (2012). Assessing the Accuracy of Georeferenced Point Clouds Produced via Multi-View Stereopsis from Unmanned Aerial Vehicle (UAV) Imagery. Remote Sensing, 4, 1573-1599

Honkavaara, E., Saari, H., Kaivosoja, J., Polonen, I., Hakala, T., Litkey, P., Makynen, J., & Pesonen, L. (2013). Processing and Assessment of Spectrometric, Stereoscopic Imagery Collected Using a Lightweight UAV Spectral Camera for Precision Agriculture. Remote Sensing, 5, 5006-5039

Kaab, A. (2002). Monitoring high-mountain terrain deformation from repeated air- and spaceborne optical data: examples using digital aerial imagery and ASTER data. Isprs Journal of Photogrammetry and Remote Sensing, 57, 39-52

Laliberte, A.S., Winters, C., & Rango, A. (2011). UAS remote sensing missions for rangeland applications. Geocarto International, 26, 141-156

Lin, A.Y.M., Novo, A., Har-Noy, S., Ricklin, N.D., & Stamatiou, K. (2011). Combining GeoEye-1 Satellite Remote Sensing, UAV Aerial Imaging, and Geophysical Surveys in Anomaly Detection Applied to Archaeology. Ieee Journal of Selected Topics in Applied Earth Observations and Remote Sensing, 4, 870-876

Lisein, J., Pierrot-Deseilligny, M., Bonnet, S., & Lejeune, P. (2013). A Photogrammetric Workflow for the Creation of a Forest Canopy Height Model from Small Unmanned Aerial System Imagery. Forests, 4, 922-944

Pierrot-Deseilligny, P., & Cléry, I. (2011). APERO, an Open Source Bundle Adjusment Software for Automatic Calibration and Orientation of a Set of Images. In, Proceedings of the ISPRS Commission V Symposium, Image Engineering and Vision Metrology. Trento, Italy

Snavely, N., Seitz, S.M., & Szeliski, R. (2008). Modeling the world from Internet photo collections. International Journal of Computer Vision, 80, 189-210

White, J.C., Wulder, M.A., Vastaranta, M., Coops, N.C., Pitt, D., & Woods, M. (2013). The Utility of Image-Based Point Clouds for Forest Inventory: A Comparison with Airborne Laser Scanning. Forests, 4, 518-536

Wolf, P.R. (1983). Elements of Photogrammetry, 2nd ed. McGraw-Hill Book Co.